arXiv:cond-mat/0409105v1 [cond-mat.str-el] 5 Sep 2004

# Infrared study of giant dielectric constant in Li and Ti doped NiO

Jung-Ho Kim[1], Youngwoo Lee[2], A Souchkov[3], J. S. Lee[4], H. D. Drew[3], S.-J. Oh[1], C.W. Nan[5] and E. J. Choi[2]
[1]*School of Physics Center for Strongly Correlated Materials Research, Seoul National University, Seoul 151-742, Republic of Korea*
[2]*Department of Physics, University of Seoul, Seoul 130-743, Republic of Korea*
[4]*Dept. of Physics, Univ. of Maryland, College Park, MD20742, USA*
[4]*School of Physics and Research Center for Oxide Electronics, Seoul National University, Seoul 151-747, Korea and*
[5]*Department of Materials Science and Engineering, Tsinghua University, Beijing 100084, China*

We have measured optical reflectivity of Li and Ti doped NiO (LTNO) in the infrared range at various temperatures. A Drude-like absorption is found at low energy, $\omega < 100$ cm$^{-1}$ and its spectral weight increases substantially as temperature decreases. This observation and DC-resistivity result show that LTNO has a conductive grain and resistive boundary. Such composite structure provides evidence of the Maxwell-Wagner (MW) mechanism as the origin of the high dielectric constant $\varepsilon_o$. We propose a three-phase granular structure and show that this extended MW model explains the observed frequency and temperature dependence of the dielectric constant as well as the giant value of $\varepsilon_o$.

PACS numbers: 63.20.-e,77.22.Ch,78.30.-j

The search for high dielectric constant ($\varepsilon_o$) materials has been driven by the continuing demand for electronic devices miniaturization. As a capacitor component, the high dielectric constant enables the reduction of the circuit size and can realize the tera-bit density static/dynamic random-access memory.[1] It is also needed as a resonator and filter in the microwave telecommunication. High $\varepsilon_o$ of $\sim$ 1000 is found in ferroelectric oxides such as $BaTiO_3$ and in dielectric relaxors such as $(Bi,Sr)TiO_3$.[2] However, in these materials, the dielectric constant is strongly temperature dependent and the application is often limited.

The finding of huge dielectric constant in $CaCu_3Ti_4O_{12}$(CCTO) has provided a new subject of study.[3,4] $\varepsilon_o$ of CCTO is high ($> 10^5$) and has small frequency and temperature dependence which are advantageous for practical use. Accumulating evidences exclude this material from the ferroelectric/relaxor category. He *et al.* made a first principle calculation of the lattice and electronic structure of CCTO but found no direct link of these intrinsic properties with the high $\varepsilon_o$.[5] As an alternative, extrinsic origin associated with the composite microstructure has been considered.[3,4,5,6,7] In the internal barrier layer capacitor (IBLC) theory, the bulk CCTO is assumed to consist of semi conductive domain and insulating boundary, caused by the twinning of the unit cell.[4] This composite capacitor structure can give rise to the high $\varepsilon_o$ in the capacitance measurement through the Maxwell-Wagner mechanism (MW). Also the decrease of $\varepsilon_o$ when Ca is replaced by Cd was understood in this picture.[8]

Recently, Wu *et al.* found that a Li and Ti co-doped NiO (LTNO) sample exhibits a giant dielectric constant.[9] The high $\varepsilon_0$ ($> 10^4$) is maintained over wide frequency range ($10^2$ Hz - $10^6$ Hz). As in the case of CCTO, $\varepsilon_0$ drops above a characteristic frequency $\Gamma(\sim 10^5$ Hz at 250 K). Even after the drop, the dielectric constant is still significant, $\sim$300. This frequency dependent behavior is described numerically by the Debye form, $\varepsilon(\omega) = \varepsilon_\infty + (\varepsilon_o - \varepsilon_\infty)/(1 - i\omega/\Gamma)$ where $\varepsilon_o$ ($\varepsilon_\infty$) represents the static (high frequency) dielectric constant. $\varepsilon_o$ is known to change with the Li and Ti concentration. As $T$ decreases, $\Gamma$ decreases drastically as $\Gamma(T) \sim e^{-U/kT}$. The high $\varepsilon_o$ is absent in NiO. Thus, a comparison of LTNO and NiO through a spectroscopic study will provide useful information on the origin of the high dielectric constant.

In this work, we have made infrared reflectivity measurement of LTNO and NiO to study the effect of Ni-site substitution on the structural and electronic properties. The infrared features we observe show that Li and Ti doping yields the IBLC structure in LTNO. Then we analyze the high dielectric constant in terms of the MW theory and find that various aspects of $\varepsilon(\omega)$ such as the $\omega$- and $T$-dependence can be coherently explained.

The $Li_{0.05}Ti_{0.02}Ni_{0.93}O$ (LTNO) and NiO pellets were prepared by the sol-gel method as described in Ref. 9. Near-normal incident reflectivity R($\omega$) was measured in the frequency range of 25 - 5000 cm$^{-1}$ using a Fourier transform spectrometor(Bomem DA8). The cubic structure of LTNO enables the probe of intrinsic property with the polycrystal samples. The sample was mounted in a closed cycle He-flow cryostat (Oxford) and the temperature was varied between 50 and 300 K.

Figure 1 shows the infrared spectra of LTNO and NiO taken at room temperature. In Fig.1(a), the reflectivity of NiO shows a typical behavior of a dielectric insulator. R($\omega$) consists of a IR-active phonon structure and a flat electronic background at low frequency. The former is composed of a transverse optical (TO) and a longitudinal optical (LO) mode of Ni-O oscillation which corre-

Typeset by REVTEX

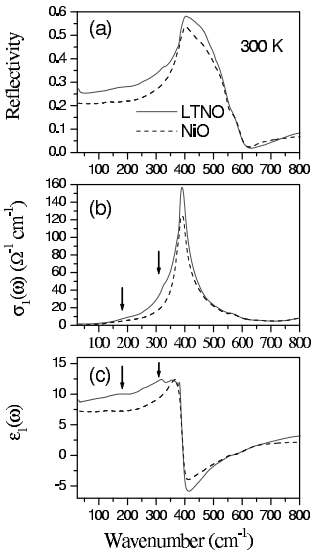



FIG. 1: Comparison of infrared spectra of LTNO and NiO: (a) Reflectivity (b) Conductivity (c) Dielectric constant

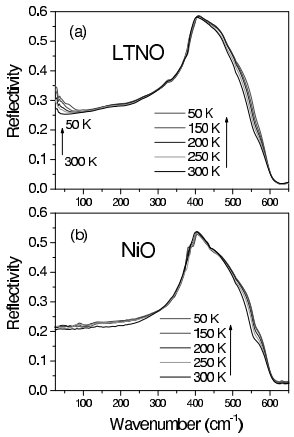



FIG. 2: Temperature dependent reflectivity of (a) LTNO and (b) NiO

sponds to the peak at 400 cm$^{-1}$ and the dip at 620 cm$^{-1}$, respectively. In LTNO, the overall structure of R($\omega$) is similar to that of NiO, except that the level is somewhat higher.[10]

From R($\omega$), we obtained the optical conductivity $\sigma_1(\omega)$ (Fig.1(b)) and the dielectric constant $\varepsilon_1(\omega)$ (Fig.1(c)) through the Kramers-Kronig transformation. Here we used a constant-reflectivity extension for the low frequency extrapolation $\omega \longrightarrow 0$. For the high frequency side, R($\omega$) was extended to 20,000 cm$^{-1}$ above which the standard form R($\omega$) $\sim \omega^{-4}$ was employed. In $\sigma_1(\omega)$, while the phonon spectra are similar in the two samples, we find that two weak structures appear at $\sim$ 320 cm$^{-1}$ and 200 cm$^{-1}$ in LTNO. These absorptions may suggest a structural distortion due to the (Li,Ti) substitution which can activate new phonon modes. In the $\varepsilon_1(\omega)$ plot, these absorptions appear as dispersive structures as indicated by the arrows. They contribute to enhance $\varepsilon_1$ but the strengths are weak and are unlikely to be related with the high $\varepsilon_o$.

Figure 2 displays R($\omega$) of LTNO and NiO at various temperatures down to 50 K. In LTNO, we find two $T$-induced changes as indicated by the arrows. As temperature decreases, the reflectivity increases continuously in the phonon region around 550 cm$^{-1}$. The other feature occurs at low frequency below $\sim$ 100 cm$^{-1}$ where a Drude-like absorption is found to grow. The former increase occurs over the Restrahlen band, $400 - 600$ cm$^{-1}$ where $\varepsilon_1(\omega) < 0$. The reflectivity level in this range depends on the phonon damping rate. At low $T$, the phonon damping is reduced and the Restrahlen band becomes more reflecting. Except this minor change, the phonon structure does not exhibit any $T$-dependent behavior in the strength and frequency. This is in clear contrast with the case of the ferroelectric materials such as $SrTiO_3$ and the cubic perovskite CCTO where the phonon peaks change drastically due to the lattice rearrangement or the charge redistribution within the unit cell.[8,11] In LTNO, therefore, the lattice effect is un- or minimally coupled with the high dielectric constant. In NiO, note that the Drude-like feature is absent, which shows that the feature is an effect of the Li / Ti doping.

Figure 3 shows this interesting low frequency absorption in an expanded scale. The feature is weak at 300 K but grows continuously with decreasing $T$ to a substantial amount. We think that this metallic feature is associated with the Li (and possibly Ti) ions which can have different electronic valency (+1 for Li) from that of Ni ion (+2). We used the Drude-Lorentz model based on the classical dispersion theory to fit R($\omega$)

$$\varepsilon(\omega) = \varepsilon_\infty + \sum_i \frac{S_i \omega_i^2}{\omega_i^2 - \omega^2 - i\gamma_i\omega} + \frac{4\pi i}{\omega}\sigma(\omega)$$

Here $\varepsilon_\infty$ represents the high frequency dielectric contribution. As for the phonon part (the second term), we followed the analysis of Gielisse *et al.* who used two sets of TO-LO modes to fit the phonon spectrum of NiO.[12] $S_i$, $\omega_i$ and $\gamma_i$ represent the oscillator strength, frequency and damping rate of the $i$-th mode. We also included two weak absorptions at 200 and 320 cm$^{-1}$. In the Drude term, $\sigma(\omega) = \omega_p^2/4\pi(\gamma - i\omega)$ represents the ac-conductivity where $\omega_p$ and $\gamma$ correspond to the plasma frequency and scattering rate, respectively. The inset shows the fitting result over a wide range. The fitting parameters are summarized in Table 1. As $T$ decreases, we find that $\omega_p$ and $\gamma$ increase. This behavior will be discussed later on. DC resistivity calculated from $\rho = 59.9 \times \gamma/\omega_p^2$ $(\Omega \cdot cm)$ shows a moderate decrease with lowering $T$, suggesting a poor metallic character of the carriers. In Eq.(1), when $\omega$ is low enough than the phonon frequencies, the first two terms can be simplified as $\varepsilon_\infty + \sum_i S_i \equiv \varepsilon_{ir}$ and Eq.(1) is reduced to

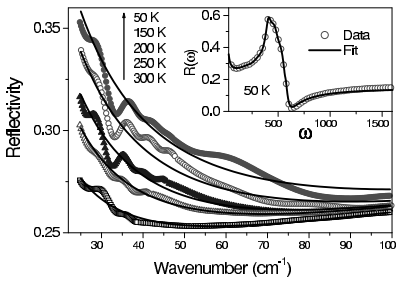



FIG. 3: T-dependence of the low frequency reflectivity. The solid lines are the fitting curves using the Drude-Lorentz model, Eq.(1). Inset: the fit over wide range of frequency for 50 K reflectivity.

$\varepsilon(\omega) = \varepsilon_{ir} + 4\pi i\sigma(\omega)/\omega$. We will use this convenient form when we discuss below the high $\varepsilon$ of the radio frequency range, $\omega < 10^6$ Hz. We take $\varepsilon_{ir} \sim 10$, the value of $\varepsilon_1$ at the low frequency limit of Fig.1(c).

In the Maxwell-Wagner theory, high dielectric constant can arise in a material with granular structure. Wu *et al.* showed that LTNO sample consists of the grains ($\sim \mu m$ in size) separated by thin boundary layer.[9] In such composite geometry, $\varepsilon(\omega)$ from the capacitance measurement is given as

$$\frac{1}{\varepsilon(\omega)} = \frac{f_g}{\varepsilon_g(\omega)} + \frac{f_b}{\varepsilon_b(\omega)} \qquad (1)$$

where $(\varepsilon_g(\omega), f_g = 1 - f_b)$ and $(\varepsilon_b(\omega),\ f_b)$ represent the complex dielectric constant and volume fraction of the grain and the boundary, respectively. With $f_b \ll 1$ the boundary contribution is negligible to the infrared reflectivity and R($\omega$) is dominated by the grain. From the effective medium theory, the infrared result $\varepsilon(\omega)$ represents the $\varepsilon_g(\omega)$.[13] As for $\varepsilon_b(\omega)$, the boundary layer is thought to be highly resistive: we measured the DC-resistivity $\rho$ of LTNO using the four point probe method.[14] At all $T$, $\rho$ was greater than the limit of the voltmeter, while $\rho \sim 1$ ($\Omega\cdot$ cm) is expected from the IR spectra (Table 1). This suggests that the current of the Drude carrier is blocked by the boundary. We have then $\varepsilon_b(\omega) = \varepsilon_{ir} + i4\pi\sigma_b/\omega$ , $\sigma_b \ll \sigma_g$. With these $\varepsilon_g(\omega)$ and $\varepsilon_b(\omega)$, we find that $\varepsilon(\omega)$ has the Debye-type $\omega$-dependence, $\varepsilon(\omega) = \varepsilon_{ir} + (\varepsilon_o - \varepsilon_{ir})/(1 - i\omega/\Gamma)$. Here the static dielectric constant $\varepsilon_o$ is given as $\varepsilon_{ir}/f_b$. If we take $f_b = 10^{-3}$, the large $\varepsilon_0 = 10^4$ is produced. On the other hand, the crossover frequency $\Gamma$ is determined by the grain conductivity. It is given approximately as the dc-value $\sigma_g(o) \equiv \sigma_g$. From $\rho = 1/\sigma_g$, we obtain $\Gamma \sim 10^{10}$ Hz at 300 K. This value is far off from the measured $\Gamma$ of Ref. 9, $\Gamma \sim 10^7$ Hz. Also, $\sigma_g$ increases as $T$ decreases, which is the opposite of the drastic decrease of the measured $\Gamma$. Moreover, for $\omega >> \Gamma$, $\varepsilon(\omega)$ converges to $\varepsilon_{ir} \sim 10$, which does not agree with the observed value $\sim 300$.[9] In this context, the two phase MW model does not explain the dielectric constant of LTNO which suggests that another ingredient should be involved.

| T(K) | 50 | 150 | 200 | 250 | 300 |
|---|---|---|---|---|---|
| $\omega_p$ (cm$^{-1}$) | 260.0 | 207.6 | 160.1 | 137.5 | 108.3 |
| $\gamma$ (cm$^{-1}$) | 287.7 | 208.7 | 144.1 | 123.6 | 98.8 |
| $\rho(\Omega\cdot$ cm) | 0.25 | 0.29 | 0.33 | 0.39 | 0.50 |

TABLE I: Fitting parameters of the Drude conductivity: $\Omega_p$=plasma frequency, $\gamma$=scattering rate. The dc resistivity $\rho$ is calculated from $\Omega_p$ and $\gamma$)(see text). $\varepsilon_\infty$=5.0 was used. The phonon parameters are omitted for brevity

Micro granular structure of oxide materials is often rather complicated. In La-doped BaTiO3, for example, the outer region of a grain is considered to have different electrical property from the interior, and forms a third layer between the grain and the grain boundary. West *et al.* used this three-layer picture to explain the dielectric response of La:$BaTiO_3$.[15,16,17] We consider this picture, among others, as a possible explanation of our case: According to a composition analysis of LTNO, Li ions are distributed within the grain but Ti ions are segregated toward the boundary.[9] We propose that they form a third layer between the grain and the boundary. This layer will be more resistive than the boundary layer: We assume that the boundary layer is bare NiO. It is known that pristine NiO has residual Ni vacancies. The dilute vacancies induce carriers (hole) which conduct through a thermally activated hopping $\sigma_b = \sigma_o e^{-U/kT}$ with $U \sim 0.1$ $eV$.[18,19] In the Ti-rich layer, the electrons from Ti ions will compensate the holes from the Ni vacancies, which makes the layer insulating ($\sigma = 0$). This layer contributes $f_I/\varepsilon_I(\omega)$ to Eq.(2) where $f_I($ << 1) and $\varepsilon_I = \varepsilon_{ir}$ represent the volume fraction and the dielectric constant, respectively.

The resulting $\varepsilon(\omega)$ is shown in Fig.4. In this simulation, we used the parameters $f_b = 3 \times 10^{-2}, f_I = 10^{-3}$ and $U = 0.3\ eV$ . In the upper panel, $\varepsilon(\omega)$ exhibits a two-step structure where $\varepsilon(0) = 10^4$ drops at $\omega = \Gamma_L$ ($10^4$ Hz), followed by another drop at higher $\omega = \Gamma_H$ ($10^{12}$ Hz). This behavior is understood from $\varepsilon(\omega)$ of the three layers, $\varepsilon(\omega) = \varepsilon_{ir} + i4\pi\sigma/\omega$ where $\sigma_g \gg \sigma_b \gg \sigma_I = 0$. When $\omega$ is high enough, $\varepsilon(\omega)$ of each layer becomes $\varepsilon_{ir}$ and so does the total $\varepsilon(\omega)$. This corresponds to the $\omega > \Gamma_H$ region. As $\omega$ decreases, the conducting term becomes comparable to $\varepsilon_{ir}$ for the grain layer, $\varepsilon_{ir} \sim 4\pi\sigma_g/\omega$ while the other two layers are still insulating. This situation corresponds to the two-component MW case of a conducting grain and an effectively single layer of boundary with a volume fraction of $f_b + f_I$. Then $\varepsilon$ in this range is given as $\varepsilon = \varepsilon_{ir}/(f_b + f_I)$. The crossover occurs when $\varepsilon_{ir} \sim \sigma_g/\omega$ which determines $\Gamma_H = \sigma_g/\varepsilon_{ir}$. Note that $\varepsilon$ is much higher than the infrared value $\varepsilon_{ir}$, $\varepsilon \sim 30 \times \varepsilon_{ir}$. This result accounts for the puzzling discrepancy of the dielectric constants from the infrared result and from the microwave result. As $\omega$ is further decreased, the crossover now occurs in the boundary layer when $\varepsilon_{ir} \sim 4\pi\sigma_b/\omega$.

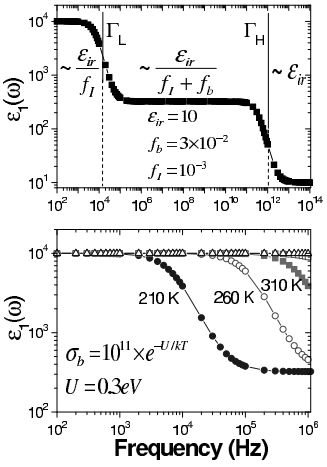



FIG. 4: Dielectric constant simulated from the three phase MW model. (a) Two step structure of $\varepsilon(\omega)$. $\Gamma_L$ and $\Gamma_H$ represent the the low and the high energy crossover frequencies respectively. (b) Shift of $\Gamma_L$ with temperature.

Then a single effective grain is formed and the MW composite has an insulating layer of $f_I$. Here $\varepsilon = \varepsilon_{ir}/f_I$ and this crossover occurs at $\Gamma_L = \sigma_b/\varepsilon_{ir}$.

Unlike $\Gamma_H$, $\Gamma_L$ exhibits a large temperature dependence. In the lower panel, we show $\varepsilon(\omega)$ for various $T$. As $T$ decreases, $\Gamma_L$ shifts rapidly due to the T-dependence of $\sigma_b$. This behavior closely reproduces the experimental results. Also, the high dielectric constant of LTNO is known to depend on the Li and Ti concentration. If Ti becomes rich, in our picture, $f_I$ tends to increase and $\varepsilon$ will decrease. On the other hand, if Li content increases, the grain becomes Li-abundant. When continued, even the boundary region will be overwhelmed by Li and the Ti-layer will become thinner. Then $f_I$ decreases and $\varepsilon$ is enhanced, consistent with the observed behavior. Although the model we have employed seems to explain the main features of the dielectric phenomena of LTNO, it certainly needs to be tested by further experiments. $\varepsilon(\omega)$ measurement to observe the drop at $\omega = \Gamma_H$ will be useful. This requires an extension of the current experimental window ( $\omega < 10^6$ Hz) to higher fequency. Also extension of the reflectivity measurement toward the lower frequency, perhaps using a terahertz spectroscopy and a resonant microwave cavity method will be interesting. Further, a direct evidence of the three layer structure using a scanning probe microscopy is desired.

The Drude carrier is quite unconventional in that the plasma frequency $\omega_p$ increases as $T$ decreases while it is conserved in normal metals. We note that NiO is a Mott-Hubbard insulator and the doped LTNO can exhibit some unusual features of the strong electron correlation origin. In a numerical study using the dynamic mean field theory, the spectral weight of the Drude conductivity ($\omega_p^2$) in a doped Hubbard system seems to grow as $T$ decreases.[20]Another unusual feature is the increase of the scattering rate $\Gamma$ with decreasing $T$ which is the opposite of the conventional behavior. This may suggest an exotic scattering mechanism in LTNO which we do not understand at this point.

In summary, we have studied the effect of Li and Ti doping in NiO through the infrared spectroscopic measurement and considered the implication on the high dielectric constant of LTNO. We find that the doping brings about a Drude carrier which coexists with a resistive grain boundary. This composite structure of electrically different media support the Maxwell-Wagner mechanism as the origin of the high $\varepsilon_o$. Our analysis showed that, however, a two phase MW model does not account for the observed behaviors of $\varepsilon(\omega)$ such as the frequency dependence. We introduced a third layer, assumed to be insulating, and showed that the three phase MW model can explain the high $\varepsilon$, the $\omega-$ and $T-$ dependence. The large discrepancy between the infrared $\varepsilon$ and the microwave $\varepsilon$ is reconciled as well. For complete understanding of this material, extension of the spectroscopic study into the intermediate region between the infrared and the microwave frequencies, $10^6$ Hz $< \omega < 10^{11}$ Hz will be interesting.

This work was supported by the Korean Science and Engineering Foundation (KOSEF)through Center for Strongly Correlated Materials Research (CSCMR). One of us(EJC) acknowledges the financial support by the KRF-2002-070-C00032. We thank useful discussions with H.-Y. Choi.

[1] A. I. Kingon, J.-P. Maria, and S. K. Streiffer, Nature (London) **406**, 1032 (2000).
[2] C. Ang, J. F. Scott, Z. Yu, H. Ledbetter, and J. L. Baptista, Phys. Rev. B **59**, 6661 (1999).
[3] M. A. Subramanian, N. D. Dong Li, B. A. Reisner, and A. W. Sleight, J. Solid State Chem **151**, 323 (2000).
[4] A. P. Ramirez, M. A. Subramanian, M. Gardel, G. Blumberg, T. V. D. Li, and S. M. Shapiro, Solid State Commun **115**, 217 (2000).
[5] L. He, J. B. Neaton, M. H. Cohen, D. Vanderbilt, and C. C. Homes, Phys. Rev. B **65**, 214112 (2002).
[6] N. Kolev, R. P. Bontchev, A. J. Jacobson, V. N. Popov, V. G. Hadjiev, A. P. Litvinchuk, and M. N. Iliev, Phys. Rev. B **66**, 132102 (2002).
[7] D. C. Sinclair, T. B. Adams, F. D. Morrison, and A. R. West, Appl. Phys. Lett. **80**, 2153 (2002).
[8] C. C. Homes, T. Vogt, S. M. Shapiro, S. Wakimoto, M. A. Subramanian, and A. P. Ramirez, Phys. Rev. B **67**, 092106 (2003).
[9] J. Wu, C.-W. Nan, Y. Lin, and Y. Deng, Phys. Rev. Lett **89**, 217601 (2002).
[10] We note that the reflectivity level is lower than the single crystal data in literature, probably due to the surface scattering and the low density of the polycrystal samples. We

have performed a high temperature, high pressure annealing of NiO which resulted in an improved density. The reflectivity became higher close to that single crystals. However, the same treatment of LTNO caused a serious chemical dissociation unfortunately, and the sample lost the structural stability.

[11] C. C. Homes, T. Vogt, S. M. Shapiro, S. Wakimoto, and A. P. Ramirez, Science **293**, 673 (2001).

[12] P. J. Gielisse, L. C. M. J. N. Plendl and, R. Marshall, S. S. Mitra, R. Mykolajewycz, and A. Smakula, J. Appl. Phys. **36**, 2446 (1965).

[13] In the effective medium approximation, $\varepsilon$ is given from $f_b(\frac{\varepsilon_b-\varepsilon}{\varepsilon_b+2\varepsilon})+(1-f_b)(\frac{\varepsilon_g-\varepsilon}{\varepsilon_g+2\varepsilon})=0$. For $f_b \ll 1$, $\varepsilon$ converges to $\varepsilon_g$. This approxiamtion holds when the wavelength of incident radiation is much larger than the grain (and boundary) size, which is valid for our infrared measurement. Note that the infrared effective dielectric constant is different from that of the effective capacitance, Eq.(2).

[14] For the four probe resistivity measurement, we used a resistance bridge of PPMS (Physical Property Measurement System, Quantum Design). This instrument has a current source (I > 10 nA) and a voltmeter (V < 1 volt) which can measure resistance up to $10^9\Omega$.

[15] A. R. West, T. B. Adams, F. D. Morrison, and D. C. Sinclair, J. Euro. Ceram. Soc. **24**, 6 (2004).

[16] S. Saha and S. B. Krupanidhi, J. Appl. Phys. **87(2)**, 15 (2000).

[17] D. C. Sinclair and A. R. West, J. Appl. Phys. **66(8)**, 15 (1989).

[18] D. Adler and J. Feinleib, Phys. Rev. B **2 (8)**, 3112 (1970).

[19] D. Snowden and H. Saltzburg, Phys. Rev. Lett **14 (13)**, 497 (1965).

[20] Private communication with H -Y. Choi.